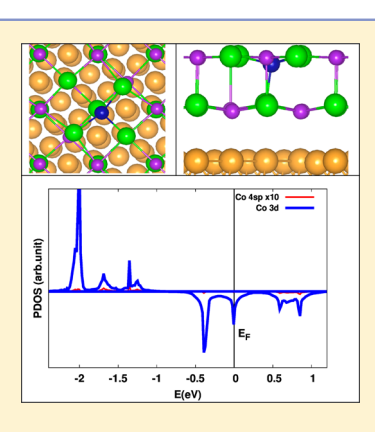
Adsorption Properties of Two-Dimensional NaCl: A Density Functional Theory Study of the Interaction of Co, Ag, and Au Atoms with NaCl/Au(111) Ultrathin Films

Hsin-Yi Tiffany Chen, Livia Giordano, and Gianfranco Pacchioni*

Dipartimento di Scienza dei Materiali, Università di Milano-Bicocca, via Cozzi 55, 20125 Milano, Italy

ABSTRACT: Recent experiments have shown that Co atoms deposited on NaCl/Au(111) ultrathin films give rise to spontaneous substitutional doping of the NaCl layer (Li et al. Phys. Rev. Lett. 2014, 112, 026102). In this work, the interaction of Co atoms deposited on NaCl/ Au(111) films is investigated by means of density functional theory calculations. Co atoms have been adsorbed on various sites of the surface of unsupported and supported two- and three-layer NaCl films; incorporation of the Co atoms in interstitial positions or replacement of Na and Cl lattice ions has also been investigated. The Co adsorption properties are compared with those of Ag and Au atoms. We found that all metal atoms interact strongly with NaCl/Au(111) films, giving rise to large structural distortions of the insulating layer. Co, Ag, or Au incorporation in interstitial positions between the first and second NaCl layers is thermodynamically preferred over adsorption on surface sites. The results show the reactivity of NaCl with Co is higher than that with Ag and Au and the large structural flexibility of ultrathin films of insulating materials grown on a metal support compared to the unsupported NaCl counterpart.



1. INTRODUCTION

Deposition of gas-phase metal atoms on the surface of insulating or semiconducting materials is a topic of interest for the investigation of the mechanisms of diffusion, nucleation, growth, and stabilization of supported metal nanoparticles. 1-4 These systems find application in a variety of advanced technologies, like the preparation of sensors or of heterogeneous catalysts, study of optical properties of nanoparticles interfaced with semiconducting materials, design of magnetic systems at the nanoscale, etc. To reach an atomic characterization of the deposited species, one has to use typical tools of surface science like X-ray photoemission spectroscopy (XPS), electron energy loss spectroscopy (EELS), scanning tunneling microscopy (STM), etc.^{5–7} Most of these techniques require the use of a conducting support, in contrast with the insulating nature of the materials normally employed as supports of metal nanoparticles in technological applications.

The need to characterize the material at an atomic level has prompted the design of new systems consisting of insulating thin films, from just one to a few atomic layers, epitaxially grown on a metal substrate.^{8,9} These systems have permitted a deep characterization of both structural and electronic properties of the support, showing in some cases the typical behavior of the corresponding bulk material and, in others, strong deviations from it. 10-13 This is related to the very low dimensionality of the film, which can result in unexpected and interesting properties.

Once the supporting insulating material is prepared, one can deposit atoms, clusters, or nanoparticles with various methods and study their properties. 14,15 Soft landing techniques guarantee that the deposited species do not produce damage on the surface, resulting in a noninvasive atom or cluster deposition. In some cases even mass-selected clusters can be deposited, producing collections of nanoclusters all having the same size (monodispersed supported particles). 16-18 The supported atoms or clusters that land on the surface can dissipate part of their thermal energy in diffusion processes that lead to particle nucleation and growth. Usually, this occurs in correspondence of specific sites (point defects, low coordinated atoms, steps, etc.) where atoms and clusters bind more strongly. 19 Usually, the atoms arriving from the gas phase remain adsorbed on the surface of the insulating material without diffusion or incorporation into the insulating thin film. Notable exceptions to this behavior are supporting films with a porous structure which offer the possibility for the deposited atoms to penetrate and diffuse into the film. This is the case for instance of Pd atoms adsorbed on ultrathin silica films. Here the atoms diffuse through the film nanopores and become stabilized at the interface between the metal support and the oxide layer.20,21

If the kinetic energy of the gas-phase atoms is too large, deposition can result in surface damage, penetration into the film, amorphization, and formation of new disordered phases. This is the case, for instance, of ion implantation, a technique where ions of a material are accelerated in an electrical field and impacted into a solid to change its physical, chemical, or electrical properties via doping by the deposited elements. Doping of insulating materials is a technologically very

Received: March 24, 2014 Revised: May 12, 2014 Published: May 21, 2014

important process that can result in completely different properties. Just to mention a few cases, induced ferromagnetism in doped insulating oxides is of great importance in the field of spintronics.²² Doping is a promising way to improve the photoabsorption properties of oxide semiconductors for harvesting solar light for applications in photocatalysis and photoelectrochemistry.^{23–26} However, doping requires incorporating small amounts of foreign elements in a host crystal and is usually achieved via wet chemistry methods.

NaCl is among the insulating materials that have been produced in the form of ultrathin film for atoms or cluster deposition. NaCl is the prototype of ionic crystals, having a very well-defined crystal structure and a wide band gap of 9 eV. NaCl ultrathin films have been widely used as inert barriers to decouple the conduction band electrons of the metal support from the valence states of adsorbed atoms (e.g., Ag, Au), 33,34 molecules, 35,36 or nanostructures (e.g., C_{60}). This has allowed the study of interesting phenomena like the selective charging and discharging of supported metal atoms by electron injection from an STM tip. 34

Recently, it has been shown that Co atoms adsorbed at low temperature on NaCl/Au(111) films do result in spontaneous doping and incorporation into the NaCl layer.³⁹ In fact, STM images combined with density functional theory (DFT) calculations have shown that Co can replace both Na and Cl ions in the first layer of the NaCl/Au(111) film. Because of their magnetic nature, the incorporated Co ions also give rise to magnetic couplings that depend on their position in the film.³⁹

In this study we report a systematic first-principles DFT investigation of the interaction of isolated Co atoms with free-standing NaCl two-layers (2L) and three-layers (3L) films and with the same films supported on Au(111). This work represents an essential complement to the selected computational results included in ref 39 and provides a clear example of the high reactivity of Co atoms with ultrathin NaCl films. For comparison, we report calculations on the adsorption of Ag and Au atoms on the same 2L NaCl unsupported films, and we show that the behavior is completely different from that of Co. On the supported NaCl/Au(111) film, on the contrary, an enhanced reactivity is found also for Ag and to a lesser extent for Au.

The paper is organized as follows. After a description of the computational setup (section 2), we first discuss Co adsorption on unsupported NaCl 2L and 3L films and we compare this with the adsorption of Ag and Au atoms (section 3.1). This is followed by a similar discussion of the energetics of Co, Ag and Au atoms adsorption and incorporation into 2L and 3L NaCl/ Au(111) films (section 3.2). Some general conclusions are reported in the final section.

2. COMPUTATIONAL DETAILS

Spin-polarized density functional theory calculations were performed using the generalized gradient approximation (PBE functional⁴⁰) and the plane waves code VASP. The interaction between the ions and the valence electrons is described by the projector augmented wave (PAW) method. As

The NaCl(001) films on Au(111) substrates have been modeled by a coincidence structure, obtained by superposing a (2×2) NaCl(100) unit cell on a $\begin{pmatrix} 3 & 1 \\ 1 & 3 \end{pmatrix}$ superstructure of the Au(111) surface.^{39,44} This coincidence structure presents a residual strain of about 5%, which is accommodated in the substrate, while the angle of the substrate unit cell is adjusted

from 82° to 90° to match the square symmetry of the NaCl film. Therefore, the same lattice parameter is used for unsupported and supported NaCl films. The metal surface is modeled by a five atomic layer thick slab. A $(6 \times 6 \times 1)$ Monkhorst–Pack grid is used for the reciprocal space sampling. The atomic coordinates of the top three layers of the Au slab and all coordinates of the NaCl films and metal atoms are fully relaxed.

Atomic charges are obtained within the scheme of charge density decomposition proposed by Bader.⁴⁵ The reported magnetic moments are the total magnetic moments per unit cell.

We have defined the adsorption energy of a metal atom M as

$$\Delta E = E(M/NaCl/Au) - E(M) - E(NaCl/Au)$$
 (1)

and the sign convention is such that $\Delta E < 0$ indicates an exothermic process.

The inclusion of van der Waals (vdW) interactions is essential in the systems considered because the adhesion of the NaCl film to the Au support is dominated by polarization and dispersion forces. vdW forces are important also for the adsorption of metal atoms on an insulating film. In this work they have been included by means of the pairwise force field as implemented by Grimme (DFT-D2).46 Of course, this approach is not free from limitations. One is the metallic screening of the dispersive interactions, which is not accounted for in the pairwise evaluation of dispersion forces, resulting in an overestimation of the interaction energies.⁴⁷ To check the role of vdW forces, we have considered the special case of a Ag atom adsorbed on a 2L NaCl/Au(111) film, and we have compared the DFT-D2 results with those of a calculation without vdW and with vdW corrections obtained from a different procedure. In particular, we followed the approach proposed by Dion et al. in which the vdW functional is expressed directly as a function of the electron density. 48 This has been later modified by Klimes et al. 49 The results are shown in Table 1. Without vdW forces, the Ag atom binds on top of a

Table 1. Binding Energy (Electronvolts) of an Ag Atom Adsorbed or Incorporated on a 2L NaCl/Au(111) Film without and with Inclusion of van der Waals Forces

	on top of Cl	interstitial	diffusion barrier
DFT^a	-0.16	-0.48	yes
vdW-DF	-0.47	-1.36	yes
DFT-D2	unstable	-1.79	no

"To avoid the detachment of the NaCl film from the substrate, the vertical position of the interfacial Cl atoms has been fixed to the value obtained for the bare 2L NaCl/Au(111) film within the DFT-D2 method.

Cl anion on the NaCl surface by -0.16 eV only. A deeper minimum, with $\Delta E = -0.48$ eV, is found if the Ag atom is included in an interstitial site of the film, between the first and second NaCl layers. The two minima are separated by a barrier (not investigated). Going to the vdW-DF method, the adsorption of Ag on top of Cl becomes -0.47 eV. Even stronger is the effect on the interstitial site where the binding is -1.36 eV, with a change of 0.89 eV due to vdW interactions. Also in this case two minima could be located, on top of Cl and interstitial, indicating the existence of a barrier. With the DFT-D2 method we find that the adsorption site on top of Cl is unstable and that the Ag atom spontaneously penetrates into

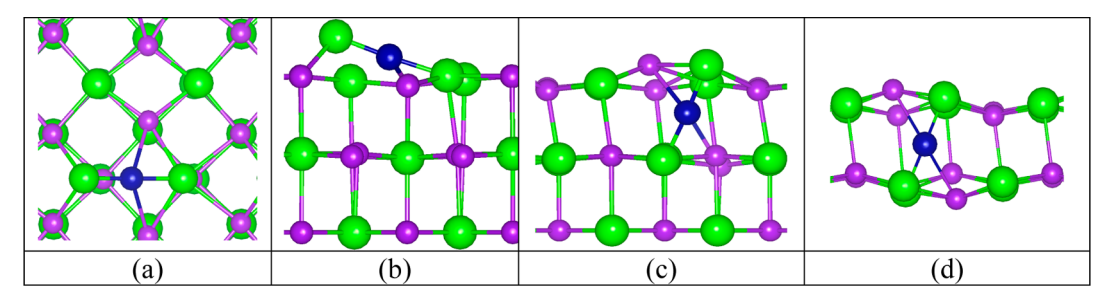


Figure 1. Structure of a Co atom adsorbed in hollow site: (a) top view and (b) side view; (c) and (d) side views of Co in an interstitial site of a 3L and 2L NaCl unsupported film, respectively. Violet, Na; green, Cl; blue, Co.

Table 2. Adsorption Energy, Magnetic Moment, μ_B , and Net Charge (Bader) for Co Atoms Adsorbed or Incorporated on Unsupported and Supported 3L and 2L NaCl Films

system		Co site	$\Delta E \text{ (eV)}$	$\mu_{ ext{B}}$	q lel
3L NaCl	adsorbed	Na-top ^a	-0.28	3.0	+0.05
	adsorbed	Cl-top ^b	-0.94	3.0	-0.05
	adsorbed	hollow ^b	-0.93	1.0	+0.02
	incorporated	$Co_{interstitial}$	-1.37	1.0	-0.03
2L NaCl	adsorbed	Cl-top ^b	-0.89	3.0	-0.03
	adsorbed	hollow ^b	-1.02	1.0	-0.08
	incorporated	$Co_{interstitial}$	-1.59	1.0	-0.13
3L NaCl/Au(111)	adsorbed	Cl-top ^b	-1.03	1.4	+0.23
	adsorbed	hollow ^b	-1.89	1.8	+0.44
	incorporated	Co _{first layer} ; Na _{first layer}	-2.05	2.0	+0.50
	incorporated	Co _{Na} ; Na _{interstitial}	-1.90	2.0	+0.66
	incorporated	Co _{Na} ; Na _{interstitial}	-2.22	2.4	+0.83
	incorporated	Co _{Na} ; Na _{interface}	-2.27	2.6	+0.86
	incorporated	Co _{Na} ; Na _{Au}	-2.58	2.5	+0.84
	incorporated	$Co_{interstitial}$	-2.60	2.0	+0.52
2L NaCl/Au(111)	adsorbed	Cl-top ^b	-1.13	1.5	+0.22
	adsorbed	$hollow^b$	-2.58	2.0	+0.48
	incorporated	Co _{Na} ; Na _{interstitial}	-2.79	2.4	+0.79
	incorporated	Co _{Na} ; Na _{interface}	-2.93	2.6	+0.91
	incorporated	$Co_{interstitial}$	-3.22	2.2	+1.00

^aNot a minimum; geometry obtained with a symmetry constraint. ^bThe Co atom is slightly tilted with respect to the surface normal.

the film, becoming stabilized at an interstitial site with $\Delta E = -1.79$ eV. So, while all three approaches indicate the interstitial site as the most stable position, significant changes in adsorption energies and even in adsorption behavior are found depending on the inclusion of vdW forces and on the method used to estimate them. Similar calculations have been performed for Co adsorbed on unsupported and supported NaCl/Au(111) films but, in contrast to the Ag case, here the results do not seem to depend on the level of treatment of the van der Waals forces.

3. RESULTS AND DISCUSSION

3.1. Metal Atom Adsorption on Unsupported NaCl Films. 3.1.1. Co Adsorption on 3L NaCl Films. The bare NaCl(001) surface was modeled by a 3L NaCl slab where only the bottom layer was kept fixed during optimization. Co has been placed on top of Na, on top of Cl, on hollow positions, and in an interstitial position between the first and second layers of the NaCl surface (Figure 1 and Table 2). Co binds on top of a Na ion with an adsorption energy of -0.28 eV, but this is not a minimum on the potential energy surface. Regarding the Cl-top adsorption site, we checked various geometries. When a symmetry constraint is imposed, Co adsorbs exactly on top of Cl with an adsorption energy of -0.73 eV. If the

symmetry constraint is released, Co is slightly off the normal to the Cl ion and the adsorption energy becomes -0.94 eV (Table 2). We also found several other nearly equivalent positions where the Co atom is slightly displaced from the surface normal, but the energy is the same within 0.02 eV. Therefore, a rapid oscillation around this position is expected even at low temperatures. The spin on Co is 3 $\mu_{\rm B}$ for the case where the Co is off-center (energetically preferred). Thus, the adsorbed Co atom keeps the same spin multiplicity as the free atom (3 unpaired electrons). The net charges on Co are very small (Table 2), indicating a substantially neutral Co atom.

Another stable configuration is found with Co sitting on hollow sites (Figure 1a,b). Also in this case we started imposing symmetry, then we removed it. With a symmetry constraint the adsorption energy is -0.86 eV; without, the atom is slightly displaced and the adsorption energy becomes -0.93 eV (Table 2). Notice that the Co atom induces a substantial distortion of the NaCl surface, with a Cl atom moving outside the surface layer. The value of the magnetization is 1 $\mu_{\rm B}$, and the charge on Co is +0.02 lel. These data clearly indicate that Co binds with very similar energies and net charges at Cl ions and hollow sites, whereas the magnetization is different.

Next we considered a case where the Co atom is incorporated into the NaCl lattice becoming stabilized in an

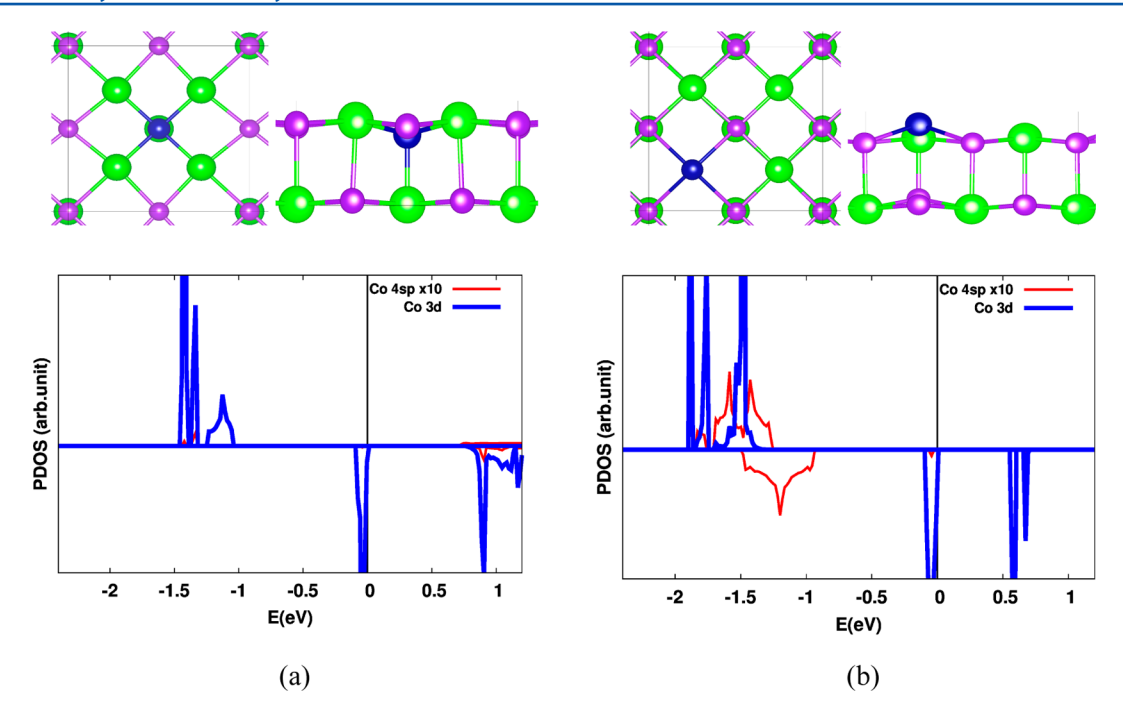


Figure 2. Structures (top and side views) and Co-projected density of states (PDOS) of unsupported 2L NaCl fims with (a) a Co atom substituting a Na lattice ion and (b) a Co atom substituting a Cl lattice ion. The zero energy represents the highest occupied state.

Table 3. Adsorption Energy, Magnetic Moment, μ_B , and Net Charge (Bader) for Ag and Au Atoms Adsorbed or Incorporated on Unsupported 2L NaCl Films

system	atom	M site		$\Delta E \; (\mathrm{eV})$	$\mu_{ ext{B}}$	q lel
2L NaCl	Ag	adsorbed	Cl-top ^a	-0.27	1.0	-0.06
		adsorbed	hollow	-0.37	1.0	-0.04
		incorporated	$Ag_{interstitial}$	0.06	1.0	-0.10
2L NaCl	Au	adsorbed	Cl-top ^a	-0.65	1.0	-0.20
		adsorbed	hollow	-0.54	1.0	-0.14
		incorporated	$Au_{interstitial}$	-0.35	1.0	-0.31
2L NaCl/Au(111)	Ag	adsorbed	hollow	-1.10	0.0	0.49
		incorporated	Ag _{interstitial}	-1.79	0.0	0.60
2L NaCl/Au(111)	Au	adsorbed	Cl-top ^a	-0.82	1.0	-0.16
		incorporated	$Au_{interstitial}$	-1.71	0.0	0.16

^aThe M atom is slightly tilted with respect to the surface normal.

interstitial site (Figure 1c). Interestingly, this turns out to be the most stable adsorption site, with an adsorption energy of -1.37 eV (spin multiplicity 1 $\mu_{\rm B}$ and the Bader charge of -0.03 lel). Also in this case we did not investigate the barrier for penetration.

3.1.2. Co Adsorption on 2L NaCl Films. Here we consider Co adsorption on a 2L NaCl unsupported film. All the atoms in the NaCl support are free to relax. As for the 3L case, adsorption on top of Na is not a minimum and will not be further discussed. Co adsorbs on top of Cl with an adsorption energy of -0.89 eV; the hollow site is slightly more stable, -1.02 eV. Thus, the two sites have adsorption energies and adsorption properties similar to those on the 3L film (Table 2). However, also in this case the most stable configuration is with the Co atom incorporated between the first and second layers of the NaCl film (Figure 1d and Table 2). The binding energy is -1.59 eV, and the lattice shows a considerable distortion (Figure 1d). The net magnetic moment is 3 $\mu_{\rm B}$ for Cl-top positions and 1 μ_B for hollow site and interstitial position (Table 2). The Bader charges are close to zero for adsorption on both surface and interstitial sites.

3.1.3. Co Substitution of Na and Cl lons in 2L NaCl Films. The last case considered is that of Co atoms replacing either Na or Cl in the unsupported 2L films (hereafter referred to as Co_{Na} and Co_{Cb} respectively; Figure 2). This is dictated by the experimental observation that by depositing Co atoms on supported NaCl films substitutional doping can be achieved.³⁹ Here no direct energetic comparison is possible with the previous cases because the number of atoms in the supercell is different, with one Na or one Cl atom missing. A free Co atom has a $4s^23d^7$ configuration. When it replaces a Na⁺ ion in the NaCl lattice it assumes the same +1 formal charge (Bader charge +0.67 lel). The electronic configuration becomes 4s⁰3d⁸, and the magnetization is 2 μ_B (five 3d_a and three 3d_b electrons). The resulting DOS curves confirm that this is the electronic configuration and that there are two empty $3d_{\beta}$ states (Figure 2a). The presence of Co at the Na position results in some structural relaxation. In particular, the in-plane Co-Cl bond lengths are 2.63 Å compared to the Na-Cl distance of 2.77 Å in the undistorted film. The interlayer Co–Cl distance is 2.40 Å (inward relaxation).

When Co replaces a Cl⁻ ion in the NaCl lattice it assumes a -1 formal charge (Bader charge -0.66 lel). The electronic configuration becomes $4s^23d^8$, and the magnetization is 2 μ_B , as for Co_{Na} (five $3d_{\alpha}$ and three $3d_{\beta}$ electrons). So, despite an opposite charge state, +1 or -1, the number of 3d electrons remains the same for both substitutional impurities. The corresponding PDOS curves show two empty $3d_{\beta}$ states and a doubly occupied 4s level (Figure 2b). Also, the presence of Co at the Cl position results in some structural relaxation. In particular, the in-plane Co–Na bond lengths are 2.93 Å (2.77 Å in NaCl; Figure 2). The interlayer Co–Na distance is 3.13 Å (outward relaxation).

To summarize this section, when Co replaces Na or Cl ions in the NaCl film, there are mainly vertical distortions in the film. The Co impurity assumes the formal charge of the substituted ion. The electronic configurations of ${\rm Co^+}$ (Na position) and ${\rm Co^-}$ (Cl position) are $4{\rm s^03d^8}$ and $4{\rm s^23d^8}$, respectively, with the same occupancy of the 3d states and the same magnetization (two unpaired 3d electrons).

3.1.4. Ag and Au Adsorption on 2L NaCl Films. In the previous sections we have shown that Co atoms bind to the NaCl surface with energies of about 1 eV and that Co incorporation into interstitial sites is energetically favorable compared to adsorption on the surface. This raises the question whether this is a general characteristic of adsorbed atoms or is specific to Co and possibly other transition metals. In order to answer this question we have considered the adsorption of Ag and Au atoms on the 2L NaCl film.

Ag and Au atoms have been placed on top of Cl, in hollow sites, or in other positions on the surface (e.g., on Na-Cl bridge sites). Ag and Au atoms in interstitial sites have also been considered (Table 3). In all cases, no symmetry constraints have been imposed. Metal adsorption on or near surface cations is unfavorable and has not been considered explicitly. Ag binds weakly on top of Cl, $\Delta E = -0.27$ eV; the Ag atom is not exactly above Cl but forms a small angle with the surface normal. In the hollow site, the adsorption energy is only slightly larger (-0.37 eV). The barriers for surface diffusion are expected to be extremely small because other local minima are found with very similar adsorption energies (around -0.3 eV). The Ag atom retains the gas-phase configuration (spin on Ag ≈ 1 ; $q \approx 0$) and no charge transfer occurs with the surface (Table 3). Incorporation of Ag into an interstitial site of the NaCl 2L film results in an unbound neutral Ag atom (Table 3). In this respect, Ag behaves completely different from Co, showing in general much weaker interaction energies and no tendency to be trapped in an interstitial site.

Au is more reactive than Ag. This is a general tendency which has been observed also for the adsorption on ionic oxides like bulk MgO^{50,51} or MgO ultrathin films. ⁵² In fact, Au binds near a Cl atom with $\Delta E = -0.65$ eV (Table 3). Also in this case the Au atom is slightly off the surface normal. When adsorbed on the hollow site, the energy is slightly higher ($\Delta E = -0.54$ eV). As for Ag, little charge transfer is found (the Au atom becomes slightly negative, and one unpaired electron occupies the Au 6s level; Table 3). Also in this case, a Au atom in an interstitial site remains neutral and is less stable than when adsorbed on the surface. However, differently from Ag, the incorporation leads to an exothermic process with $\Delta E = -0.35$ eV (Table 3).

To summarize, Ag and Au exhibit a very different behavior from Co. Both Ag and Au prefer to be adsorbed on the surface rather than to go in an interstitial site. Both Ag and Au exhibit an interaction with NaCl weaker than that of Co, a fact that is related to the specific nature of transition-metal atoms and their capability to form chemical bonds.

3.2. Metal Atom Adsorption on Supported NaCl/ Au(111) Films. 3.2.1. Co Adsorption on 3L NaCl/Au(111) Films. Co is weakly bound on top of a Na ion of the supported NaCl film and will not be further discussed. For Co on top of Cl (no symmetry constraint), the adsorption energy is -1.03eV, only slightly larger than that on the corresponding unsupported NaCl film (-0.94 eV; Table 2). This site, however, is probably not a minimum or, if it is a minimum, is separated by a tiny barrier (≈0.02 eV) from another much more stable minimum, the hollow site. Given the registry of the 3L NaCl film with the Au(111) support, in our model there are two nonequivalent hollow sites. In the first case, Co is directly above a Au-Au bridge site; in the second case, Co is directly above a Au atom of the support. Both these sites have been investigated, but because their properties are identical, only one is discussed here (see Figure 3).

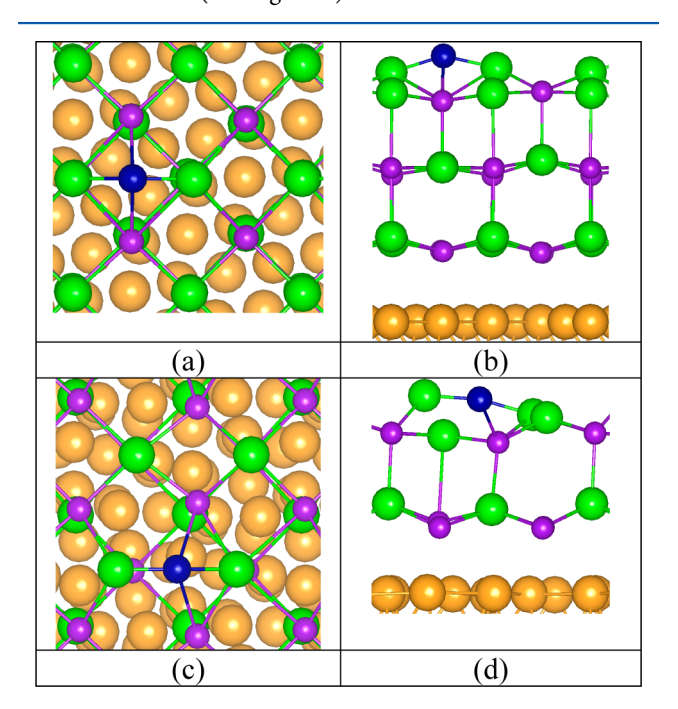


Figure 3. (a) Top view and (b) side view of Co adsorbed on the hollow site of a 3L NaCl/Au(111) film. (c) Top view and (d) side view of Co adsorbed on the hollow site of a 2L NaCl/Au(111) film.

In the hollow site the Co adsorption energy almost doubles and becomes -1.89 eV. On this site Co is 0.86 eV more stable than on top of Cl. A strong distortion is observed (Figure 3). Co is in a bridge position between two Cl ions of the surface. The value of the magnetization on Co is $1.76~\mu_{\rm B}$, and the Bader charge is +0.44 lel, indicating partial oxidation.

The pronounced structural distortion is a consequence of the strong binding of Co with the film. The supported film is therefore much more reactive than the unsupported film. Notice also that the large energy difference between the hollow site (surface global minimum) and the on-top Cl site (local minimum) suggests a larger thermal stability of the adsorbed Co atoms and probably higher diffusion barriers compared to those of the unsupported NaCl films.

3.2.2. Co Incorporation on 3L NaCl/Au(111) Films. Here we consider cases where the Co atom is incorporated into the

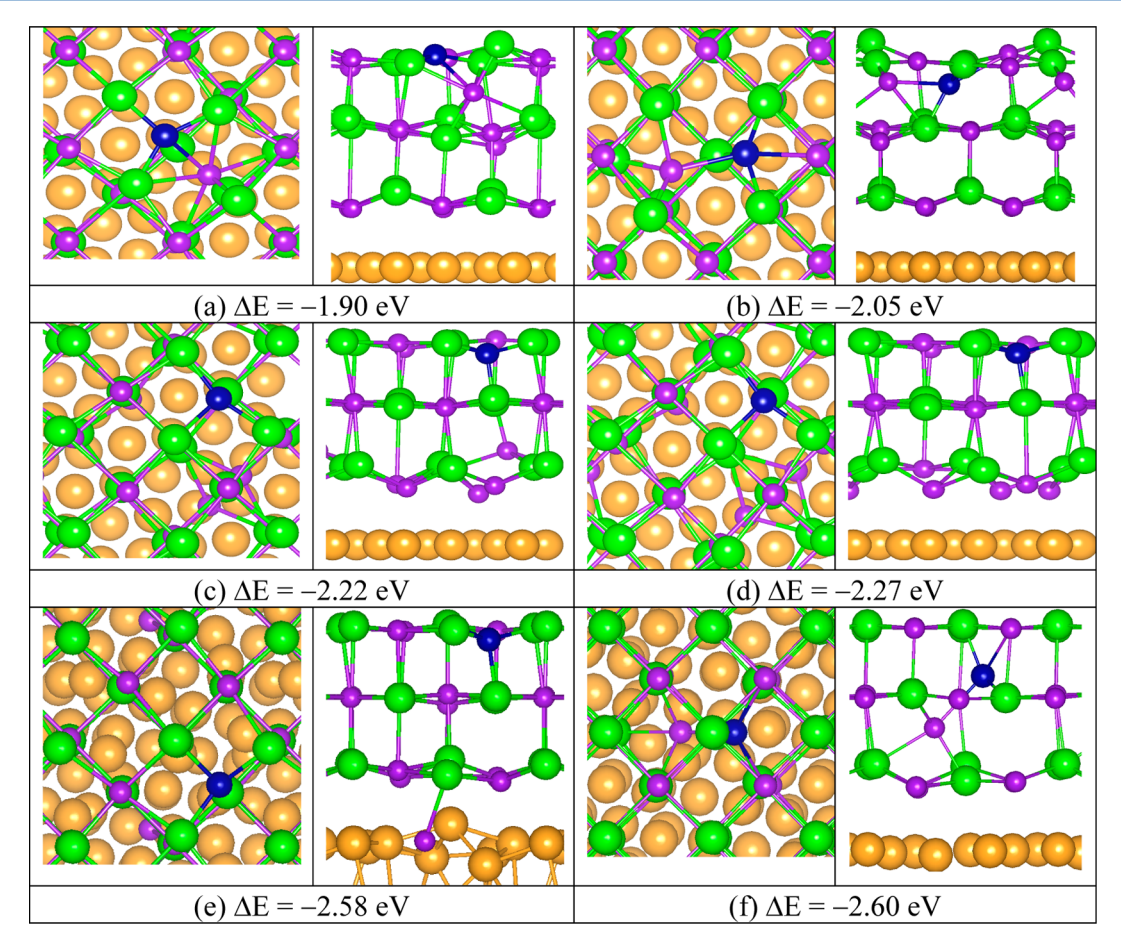


Figure 4. Top and side views of a Co atom adsorbed in various positions of a 3L NaCl/Au(111) film. (a) Co_{Na} with Na in interstitial position between first and second NaCl layers; (b) Co_{Na} with Na displaced laterally but still in 1st layer of NaCl; (c) Co_{Na} with Na in interstitial position between second and third NaCl layers; (d) Co_{Na} with Na at the NaCl interfacial layer; (e) Co_{Na} with Na incorporated in the Au support; (f) Co interstitial with a lattice Na atom displaced to another interstitial site (and formation of a Na vacancy). The total energy difference ΔE with respect to a Co atom in gas phase and NaCl/Au is reported.

NaCl film either substituting the Na ion (Co_{Na}) or going to an interstitial ($Co_{interstitial}$). We performed a set of calculations in which the total number of atoms in the supercell is conserved so that the total interaction energies ΔE , see eq 1, can be directly compared. They are reported in Figure 4 together with some structural information.

We found a number of structures where Co can replace a Na lattice ion, $\mathrm{Co_{Na}}$. This is because of two factors: (1) the displaced Na atom can occupy different positions; and (2) even for a given position occupied by Co and Na atoms, multiple minima exist. If Co replaces Na, the Na atom can go into an interstitial position between the first and the second NaCl layers, between the second and the third NaCl layers, at the NaCl interfacial layer, or on the top layer of the Au support (Figure 4a–e). Another possibility, not investigated here, is that the Na atom is simply displaced to the borders of the NaCl islands that form on the surface of $\mathrm{Au}(111)$.

The calculations indicate that the most stable configuration is with Na stabilized at the NaCl/Au interface (Figure 4e). Here the Co adsorption energy is -2.58 eV. In all cases the magnetization is $2-2.5~\mu_{\rm B}$ and the charge on Co is positive, +0.5/+0.9 lel. Even more stable, $\Delta E = -2.60$ eV, is a case where the Co atom goes interstitial and pushes a Na atom out of its lattice position (Figure 4f). The displaced Na atom goes to another interstitial site, leaving behind a Na vacancy (Figure 4f). Notice that all the cases considered, with the exception of

 ${\rm Co_{Na}}$ with Na incorporated into the Au support (Figure 4e), induce substantial distortions in the NaCl lattice. These distortions result not only in vertical displacements of the Na and Cl ions of the film but also in lateral displacements. These distortions are not observed experimentally. STM images show that the NaCl lattice essentially unperturbed upon Co incorporation. This indicates that when Co takes a Na lattice position, the displaced Na atom is far from the Co dopant.

These results show that Co has such a high affinity for the supported NaCl film that it tends to take the position of Na and be incorporated in the lattice (formally becoming Co⁺). The Na atom is then displaced into an interstitial cavity, or it can diffuse to the Au substrate with additional energy gain and reduction of the strain in the film. The barriers for diffusion have not been determined. However, in some cases, the atomic displacement is nonactivated and just follows Co adsorption. Furthermore, the energy released by Co adsorption, close to 2.5 eV per atom, is sufficiently large to overcome significant diffusion barriers. Because these phenomena depend also on the level of description of vdW forces (see section 2), further work is necessary to better identify the presence of activation barriers for atom incorporation and the extent of these barriers.

In summary, for a supported 3L NaCl/Au(111) film, Co adsorption above the surface is not the best adsorption site. The most stable configuration is either with Co replacing Na in the lattice or with Co in interstitial sites.

Figure 5. Side views of a 2L NaCl/Au(111) film with a Co incorporated in the structure. (a) Co atom in a Na lattice position, Co_{Na} ; the Na lattice atom is displaced to an interstitial site. (b) Co atom in a Na lattice position, Co_{Na} ; the Na lattice atom is displaced to the NaCl/Au interface. (c) Co atom in an interstitial site. (d) Co atom in a Cl lattice position, Co_{Cl} ; the Cl atom is removed from the supercell; notice that in this case the total number of atoms in the supercell is different from the previous cases and $\Delta E'$ is defined with respect to the formation of 1/2 Cl₂ (see eq 2).

3.2.3. Co Adsorption on 2L NaCl/Au(111) Films. Here we consider the 2L NaCl/Au(111) film, and we start discussing the properties of Co adsorbed on the hollow sites because these are preferred on the surface of unsupported and supported 3L NaCl films (Table 2). On the hollow sites of the NaCl/Au 2L film, Co is bound even more strongly than on the 3L films (Table 2). The binding energy goes from −1.89 eV (3L) to -2.58 eV (2L) and is the same in the two nonequivalent hollow sites (see above), showing that in our model the position of the NaCl layer with respect to the Au(111) support is not relevant for the Co adsorption properties. Also in this case Co is in a bridge position between two Cl ions, and the distortion of the NaCl film is even stronger than on the 3L film (compare panels b and d of Figure 3). The magnetization (2.01 $\mu_{\rm B}$) and the charge on Co (+0.48 lel) are similar to those on the 3L NaCl/Au(111) system (Table 2). A second minimum, higher in energy, is found for Co adsorbed on top of a Cl atom of the surface, with a binding energy of -1.13 eV. However, the most stable site is when Co is incorporated in the NaCl film.

To investigate the stability of incorporated Co atoms, we have considered several structures. The most relevant ones are summarized in Figure 5. Notice that the energies of these systems have to be compared to that of Co adsorbed on the hollow surface site, most stable adsorption site at the film surface (Figure 3b; adsorption energy of -2.58 eV; Table 2).

Co_{Na} with Na in the interstitial site has an adsorption energy of -2.79 eV (Figure 5a). The magnetization on Co is 2.43 $\mu_{\rm B}$, and the Bader charge is +0.79 lel (Table 2), suggesting ionization of the Co atom. In a second structure, Na diffuses to the Au support (Figure 5b) and ΔE is -2.93 eV. In both cases the energy is lower than that of an adsorbed Co atom on the hollow surface site. Even more stable is the case where Co enters in the film and becomes stabilized in an interstitial position ($\Delta E = -3.22$ eV; Figure 5c). The three energy gains computed for these rather different situations are all close to about 3 eV, and a final definition of the most stable site is not possible as it can depend also on some details of the calculations like size of the supercell, strain in the Au(111) supporting layer, method used to include vdW interactions, etc. In general, one can conclude that a Co atom incorporated in the 2L NaCl supported film is always more stable than one incorporated on its surface.

Quite different is the case of replacement of a lattice Cl ion by Co (Figure 5d). We have performed a series of calculations where a Co_{Cl} ion was included in the lattice and a Cl atom was placed in various positions of the film. However, in contrast to Na, Cl in interstitial sites or at the NaCl/Au interface is not stable. When Cl is placed at the NaCl/Au interface, it moves back into the NaCl film where it replaces the substitutional Co_{Cl} atom that goes back in the hollow adsorption position.

This is consistent with the fact that Cl is weakly adsorbed on the Au(111) surface (by about -0.9 eV). ⁵³ Also interstitial Cl is not particularly stable and tends to induce complex reconstructions of the film. This indicates that Co replacing Cl with Cl remaining inside the film is much less stable than Co replacing Na.

We have also considered the possibility that the displaced Cl atom combines with another Cl atom and desorbs as gas-phase Cl₂. In this case the reaction would be

$$Co(g) + NaCl/Au(111) \rightarrow Co_{Cl}NaCl_{1-x}/Au(111) + x/2Cl_{2}(g)$$
(2)

However, this process is unfavorable; $\Delta E' = +1.68 \text{ eV}$ (Figure 5d). This is because the cost of forming a Cl vacancy is very high and is not compensated by the formation of a Cl_2 molecule and by the inclusion of Co into the vacancy. Another possibility considered is that when Co replaces Cl, the displaced Cl atom remains adsorbed on the surface. When we start the optimization with Cl adsorbed on the surface, the system evolves to a structure where Co is no longer substitutional but becomes interstitial and Cl takes the original position (Figure 5c).

The stability of Co atoms replacing Na and Cl atoms of the 2L NaCl/Au film, followed by formation of a new NaCl film unit, can be explained considering the equation

$$\begin{split} &2\text{Co(g)} + 2\text{NaCl/Au(111)} \\ &\rightarrow \text{Co}_{\text{Na}}\text{Na}_{1-x}\text{Cl/Au(111)} + \text{Co}_{\text{Cl}}\text{NaCl}_{1-x}/\text{Au(111)} \\ &+ 1 \text{ NaCl unit} \end{split} \tag{3}$$

We found that the energy drops by 4.14 eV after two Co atoms replace one Na and one Cl atom of the 2L NaCl/Au(111) film and form an extra NaCl unit. Thus, Co substitutional incorporation at both Na and Cl sites with formation of a new NaCl unit and growth of the NaCl island is thermodynamically favorable.

The results presented above, together with direct experimental evidence, indicate that Co atoms deposited from the gas-phase on a 2L NaCl/Au(111) film can replace Na (more favorable) or Cl (less favorable) in the lattice or penetrate into the film and become stabilized in an interstitial site (not observed experimentally). Energy considerations and statistical analyses of the STM images indicate that Na substitution is preferred with respect to Cl substitution. In the case of Na substitution, we have also considered the possibility that the Co atom replaces a Na ion in the second layer of the NaCl film, being stabilized at the NaCl/Au interface. The calculations, however, indicate that structures with $\rm Co_{Na}$ in first or second NaCl layers are almost isoenergetic ($\rm Co_{Na}$ in the interface layer is 0.06 eV more stable than in the top layer). Other direct

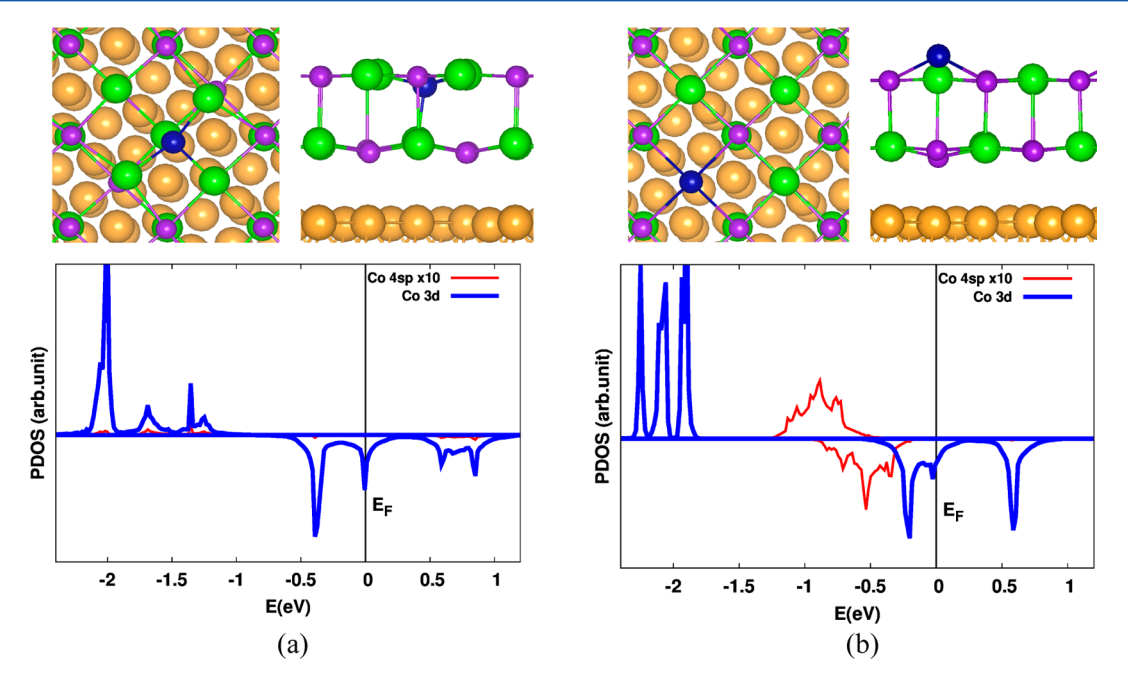


Figure 6. Structures (top panels) and Co projected density of states (PDOS) (bottom panel) of (a) 2L NaCl/Au(111) films with Co substituting Na (Co_{Na}) and (b) 2L NaCl/Au(111) films with Co substituting Cl (Co_{Cl}).

evidence coming from comparison of simulated or measured STM images provides unambiguous evidence that under the experimental conditions Co replaces Na ions only in the surface layer.³⁹

3.2.4. Electronic Structure of Co Atoms Replacing Na or Cl in 2L NaCl/Au(111) Films. We have seen above that $\mathrm{Co_{Na}}$ and $\mathrm{Co_{Cl}}$ substitutional impurities in unsupported NaCl films give rise to Co ions in formally +1 and -1 oxidation states, respectively. On an insulating layer grown on a metal, the situation could change drastically because of the possibility of exchanging electronic charge to or from the d states of the transition-metal impurity and the Fermi level of the metal support. This has been shown recently for the case of Mo ion impurities in CaO films. S4-S6 In this respect, the electronic configurations found for $\mathrm{Co_{Na}}$ or $\mathrm{Co_{Cl}}$ impurities in unsupported NaCl films could differ from those of the same atoms in the supported layers.

Here we consider explicitly the nature of Co_{Na} and Co_{Cl} species in the 2L NaCl/Au(111) films. The undoped NaCl film is weakly bound to the Au support, and another question is whether the incorporation of Co impurities in the lattice will reinforce the interaction with the metal support. However, this is not the case, and the interface NaCl—Au distance does not change significantly upon Co incorporation. This is already an indication that only moderate electron transfer occurs between the Co dopant and the Au support. In fact, in this case the resulting electrostatic interaction between charged units should lead to a major contraction of the distance. However, we found a reduction of about 0.1 Å of the Na—Au distance and an elongation of about 0.2 Å of the Cl—Au distance. The reason can be rationalized by the analysis of the DOS curves, see Figure 6 and the following discussion.

On the supported NaCl/Au(111) 2L film, Co_{Na} (Bader charge +0.92 lel) induces a modest structural distortion (Figure 6a). There are three short in-plane Co–Cl bonds of 2.38–2.39 Å and one long in-plane Co–Cl bond of 3.26 Å. The Co–Cl interlayer distance is 2.29 Å. The electronic configuration remains $4s^03d^8$, and the magnetization on Co, 2.6 μ_B , is higher

than that in the unsupported case, 2.0 μ_B , probably because of some hybridization with the tails of the Au metal wave function. In the DOS curves (Figure 6), one can identify five occupied $3d_{\alpha}$ and three occupied $3d_{\beta}$ states. These states are well below the Fermi level of the Au(111) support. The two empty $3d_{\beta}$ states are at about 0.6 and 0.85 eV above the Fermi level (Figure 6a). Thus, E_F of Au(111) lies between the occupied and the empty states of the Co ion, and no electron transfer occurs.

Co_{Cl} (Bader charge, -0.40 lel) induces some local lattice relaxation, and a Co protrusion is observed (Figure 6b). The Co–Na (top layer) bond lengths are 3.02 Å; the interlayer Co–Na distance is 4.20 Å. The electronic configuration is $4s^23d^8$; the magnetization, 2.3 μ_B , is slightly higher than that in the unsupported case. In the DOS curves one can identify five occupied $3d_{\alpha}$, three occupied $3d_{\beta}$ states, and a doubly occupied Co 4s state as for the unsupported film. The presence of the 4s level of Co below E_F is consistent with the $4s^23d^8$ configuration and with the negative charge on Co. As for Co_{Cl}, there are two empty $3d_{\beta}$ states, both at about 0.6 eV above E_F (Figure 6b).

A direct comparison of PDOS curves for Co_{Na} and Co_{Cl} with measured scanning tunneling spectroscopy spectra has been discussed in ref 39. The empty states in the PDOS appear at lower energies when compared to the experiment, i.e., around 0.6 and 0.85 eV 57 for Co_{Na} and around 0.6 eV for $\text{Co}_{\text{C}\nu}$ while the experimental peaks are at 2.2 and 1.8 eV, respectively. This is not surprising because the NaCl band gap (9 eV) is considerably underestimated in our DFT-GGA approach (5 eV). This is also the case for localized 3d states of transitionmetal atoms where the separation between filled and empty 3d states is typically underestimated in standard DFT calculations. This discrepancy, however, does not affect the interpretation of the experiments. The PDOS curves (Figure 6) reveal that the empty Co 3d states for Co_{Cl} appear at a lower energy compared to that of Co_{Na}, in agreement with the experimental $observations. \\^{39}$

3.2.5. Ag and Au Adsorption on 2L NaCl/Au(111) Films. In this section we consider the adsorption properties of Ag and Au

Figure 7. Side views of a 2L NaCl/Au(111) film with a Ag or Au atom adsorbed or incorporated in the structure. (a) Ag atom in a hollow site; (b) Ag atom in interstitial position; (c) Au atom on top of Cl site; (d) Au atom in interstitial position.

atoms on the 2L NaCl/Au(111) supported films. The atoms have been placed in three initial positions, i.e., on top of Cl, in the hollow sites of the NaCl surface, and in the interstitial sites (Table 3 and Figure 7). The response of the NaCl film to Ag and Au adsorption is quite different compared to that of the unsupported case.

The adsorption of Ag on 2L NaCl/Au(111) is much stronger than that on bare NaCl. This is well-demonstrated by the adsorption on the hollow site: on the unsupported film this is the most stable site, with an adsorption energy of -0.37 eV; on the supported film, the adsorption energy becomes -1.10 eV, i.e., three times larger in absolute value. This is because the bonding mechanism is completely different. On the supported film, Ag becomes Ag⁺. This is demonstrated by (1) the absence of magnetization on the atom, (2) the net positive Bader charge (+0.49 lel), and (3) the DOS plot that shows that the Ag 5s level is above the Fermi level of the system. Even more interesting is the fact that while in the unsupported film Aginterstitial is unbound (by 0.06 eV), on the supported film it becomes the most stable configuration with an adsorption energy of -1.79 eV. Also in this case the Ag interstitial species is ionized and forms a Ag+ ion (Table 3). The higher structural flexibility of the supported NaCl film leads to a stronger bonding and a reversal order of the stability of the two sites (hollow and interstitial). This is further demonstrated by adsorption of Ag on top of Cl: while on the unsupported film this is a local minimum, on NaCl/Au the structure of the interstitial site is 0.89 eV (Table 1) more stable than that atop Cl. The existence of the barrier depends on the level of treatment of vdW forces (see section 2). Substitution of lattice Na ions with Ag is also not excluded but has not been considered explicitly.

We consider now Au. The most stable adsorption site is near Cl, with Au forming the usual tilt angle (Table 3 and Figure 7). This is found starting the geometry optimization with Au on top of Cl or in the hollow site. The adsorption energy changes slightly going from the unsupported NaCl film (-0.65 eV) to the supported one (-0.82 eV; Table 3). The reason is simple: in this case the nature of the adsorbate is similar in the two cases as Au remains neutral on both supports (spin ≈ 1 , $q \approx$ -0.2). No tendency of the film to reconstruct and allow the spontaneous penetration of Au is observed. However, if we placed Au in the interstitial cavities of NaCl, we found a stable configuration with an adsorption energy of -1.71 eV. This is larger than the adsorption energy on the surface and indicates that interstitial Au is the most stable structure, at variance with the unsupported film where incorporation is less favorable than adsorption (Table 3). This change in stability is accompanied by a corresponding change in bonding mode; in fact, Au in interstitial sites tends to lose the valence electron and become

positively charged (Table 3). The charge transfer is not as large as in the Ag case. Notice that the fact that Ag and Au atoms adsorbed on NaCl/Au(111) films are more stable in interstitial sites does not necessarily mean that these are the sites that will be observed experimentally. In fact, the penetration of the atoms into the interstitial sites may imply overcoming an energy barrier, and their incorporation into the NaCl film may depend on the experimental deposition conditions, in particular, temperature and pressure.

In summary, both Ag and Au exhibit completely different behaviors on the free-standing and on the supported NaCl layers. The origin of this different reactivity lies in the possibility exchanging electrons between the Ag and Au atoms and the support and in the higher deformations observed in the NaCl structure supported on the Au metal.

4. CONCLUSIONS

We have performed an extensive series of calculations on the adsorption properties of Co atoms deposited on NaCl/Au(111) ultrathin films. The theoretical work is stimulated by some recent observations related to the incorporation of Co atoms deposited from the gas phase into this support. For comparison, we have considered Co adsorption on supported and unsupported NaCl films as well as Ag and Au adsorption on the same substrates.

Two main conclusions emerge from this study. The first one is that a transition-metal atom like Co interacts with the ionic NaCl substrate, forming bonds stronger than those of Ag and Au. The higher reactivity of Co is shown by the tendency of Co to bind more strongly in interstitial sites of a 2L NaCl film than to the surface sites, while Ag and Au do not show this behavior. This can be related to the nature of transition-metal atoms with incomplete d shells that favor both formation of covalent bonds and change in oxidation state of the metal atoms. Of course, also the size of the Co, Ag, and Au atoms is different and contributes to the different behaviors of the three metal atoms.

The reactivity of Co is even more pronounced on the supported NaCl/Au(111) ultrathin films. A series of structures is found where Co can enter the film in various positions also displacing Na lattice ions and resulting in spontaneous substitutional doping. Much less favorable is the case where Co replaces Cl ions in the lattice. A tendency to be adsorbed in interstitial sites is shown by Ag and, to a lesser extent, by Au, but the interaction energies are much smaller than in the case of Co.

The second general conclusion is related to the special nature of two-dimensional insulating materials deposited on a metal support. In fact, the supported NaCl layers are much more reactive than the unsupported ones. This is true for Co as well as for Ag and Au atoms. In particular, strong distortions occur

on the supported films that favor the incorporation of the metal atoms. The NaCl film by no means behaves as a rigid solid surface but exhibits strong relaxations typical of molecular systems. The high structural flexibility of the NaCl layers is reminiscent of that found for other materials like FeO/Pt(111) films that can undergo strong structural rearrangements once exposed to gas-phase molecules at high pressures. In this respect, the results presented in this work represent just another example of the uncommon nature of supported ultrathin films and of the potential that they offer for the design of new materials at the nanoscale. ^{8,9}

AUTHOR INFORMATION

Corresponding Author

*E-mail: gianfranco.pacchioni@unimib.it. Tel.: +39-2-64485219.

Notes

The authors declare no competing financial interest.

ACKNOWLEDGMENTS

We thank Dr. M. Trioni, Zhe Li, Koen Schouteden, Ewald Janssens, and Peter Lievens for very useful discussions. Financial support from the Italian MIUR through the FIRB Project RBAP115AYN is gratefully acknowledged.

REFERENCES

- (1) Libuda, J.; Freund, H. J. Molecular Beam Experiments on Model Catalysts. *Surf. Sci. Rep.* **2005**, *57*, 157–298.
- (2) Salmeron, M.; Schlogl, R. Ambient Pressure Photoelectron Spectroscopy: A New Tool for Surface Science and Nanotechnology. *Surf. Sci. Rep.* **2008**, *63*, 169–199.
- (3) Somorjai, G. A.; Park, J. Y. Molecular Surface Chemistry by Metal Single Crystals and Nanoparticles from Vacuum to High Pressure. *Chem. Soc. Rev.* **2008**, *37*, 2155–2162.
- (4) Bell, A. T. The Impact of Nanoscience on Heterogeneous Catalysis. *Science* **2003**, 299, 1688–1691.
- (5) Goodman, D. W. Catalysis: From Single-Crystals to the Real-World. Surf. Sci. 1994, 299, 837–848.
- (6) Freund, H. J. Clusters and Islands on Oxides: From Catalysis via Electronics and Magnetism to Optics. Surf. Sci. 2002, 500, 271–299.
- (7) Henry, C. R. Surface Studies of Supported Model Catalysts. Surf. Sci. Rep. 1998, 31, 231–325.
- (8) Oxide Ultrathin Films: Science and Technology; Pacchioni, G.; Valeri, S., Eds.; Wiley-VCH: Weinheim, 2012.
- (9) Pacchioni, G. Two-Dimensional Oxides: Multifunctional Materials for Advanced Technologies. *Chem.—Eur. J.* **2012**, *18*, 10144–10158.
- (10) Pacchioni, G.; Freund, H. J. Electron Transfer at Oxide Surfaces. The MgO Paradigm: from Defects to Ultrathin Films. *Chem. Rev.* (Washington, DC, U.S.) 2013, 113, 4035–4072.
- (11) Pacchioni, G.; Giordano, L.; Baistrocchi, M. Charging of Metal Atoms on Ultra-Thin MgO/Mo(100) Films. *Phys. Rev. Lett.* **2005**, *94*, 226104.
- (12) Freund, H. J.; Pacchioni, G. Oxide Ultra-Thin Films on Metals: New Materials for the Design of Supported Metal Catalysts. *Chem. Soc. Rev.* **2008**, *37*, 2224–2242.
- (13) Giordano, L.; Pacchioni, G. Oxide Films at the Nanoscale: New Structures, New Functions, and New Materials. *Acc. Chem. Res.* **2011**, 44, 1244–1252.
- (14) Chen, M. S.; Goodman, D. W. The Structure of Catalytically Active Gold on Titania. *Science* **2004**, *306*, 252–255.
- (15) Bäumer, M.; Freund, H.- J. Metal Deposits on Well-Ordered Oxide Films. *Prog. Surf. Sci.* **1999**, *61*, 127–198.
- (16) Wallace, W. T.; Whetten, R. L. Coadsorption of CO and O₂ on Selected Gold Clusters: Evidence for Efficient Room-Temperature CO₂ Generation. *J. Am. Chem. Soc.* **2002**, *124*, 7499–7505.

- (17) Hagen, J.; Socaciu, L. D.; Elijazyfer, M.; Heiz, U.; Bernhardt, T. M.; Wöste, L. Coadsorption of CO and O₂ on Small Free Gold Cluster Anions at Cryogenic Temperatures: Model Complexes for Catalytic CO Oxidation. *Phys. Chem. Chem. Phys.* **2002**, *4*, 1707–1709.
- (18) Schlangen, M.; Schwarz, H. Probing Elementary Steps of Nickel-Mediated Bond Activation in Gas-Phase Reactions: Ligand- and Cluster-Size Effects. *J. Catal.* **2011**, 284, 126–137.
- (19) König, T.; Simon, G. H.; Martinez, U.; Giordano, L.; Pacchioni, G.; Heyde, M.; Freund, H.-J. Direct Measurement of the Attractive Interaction Forces on F⁰ Color Centers on MgO(001) by Dynamic Force Microscopy. *ACS Nano* **2010**, *4*, 2510–2514.
- (20) Baron, M.; Stacchiola, D.; Ulrich, S.; Nilius, N.; Shaikhutdinov, S.; Freund, H.-J.; Martinez, U.; Giordano, L.; Pacchioni, G. Adsorption of Au and Pd Atoms on Thin SiO₂ Films: The Role of Atomic Structure. *J. Phys. Chem. C* **2008**, *112*, 3405–3409.
- (21) Ulrich, S.; Nilius, N.; Freund, H. J.; Martinez, U.; Giordano, L.; Pacchioni, G. Evidence for a Size-Selective Adsorption Mechanism on Oxide Surfaces: Pd and Au Atoms on SiO₂/Mo(112). *ChemPhysChem* **2008**, *9*, 1367–1370.
- (22) Dietl, T. A Ten-Year Perspective on Dilute Magnetic Semiconductors and Oxides. *Nat. Mater.* **2010**, *9*, 965–974.
- (23) Chen, X.; Mao, S. S. Titanium Dioxide Nanomaterials: Synthesis, Properties, Modifications, and Applications. *Chem. Rev.* (Washington, DC, U.S.) **2007**, 107, 2891–2959.
- (24) Thompson, T. L.; Yater, J. T., Jr. Surface Science Studies of the Photoactivation of TiO₂New Photochemical Processes. *Chem. Rev.* (Washington, DC, U.S.) **2006**, 106, 4428–4453.
- (25) Fujishima, A.; Zhang, X.; Tryk, D. A. TiO₂ Photocatalysis and Related Surface Phenomena. *Surf. Sci. Rep.* **2008**, *63*, 515–582.
- (26) Henderson, M. A. A Surface Science Prospective on TiO₂ Photocatalysis. *Surf. Sci. Rep.* **2011**, *66*, 185–297.
- (27) Strehlow, W. H.; Cook, E. L. Compilation of Energy Band Gaps in Elemental and Binary Compound Semiconductors and Insulators. *J. Phys. Chem. Ref. Data* **1973**, *2*, 163–199.
- (28) Wagner, M.; Negreiros, F. R.; Sementa, L.; Barcaro, G.; Surnev, S.; Fortunelli, A.; Netzer, F. P. Nanostripe Pattern of NaCl Layers on Cu(110). *Phys. Rev. Lett.* **2013**, *110*, 216101.
- (29) Repp, J.; Meyer, G.; Paavilainen, S.; Olsson, F. E.; Persson, M. Scanning Tunneling Spectroscopy of Cl Vacancies in NaCl Films: Strong Electron-Phonon Coupling in Double-Barrier Tunneling Junctions. *Phys. Rev. Lett.* **2005**, *95*, 225503.
- (30) Cabailh, G.; Henry, C. R.; Barth, C. Thin NaCl Films on Silver (001): Island Growth and Work Function. *New J. Phys.* **2012**, *14*, 103037.
- (31) Bombis, C.; Ample, F.; Mielke, J.; Mannsberger, M.; Villagomez, C. J.; Roth, C.; Joachim, C.; Grill, L. Mechanical Behavior of Nanocrystalline NaCl Islands on Cu(111). *Phys. Rev. Lett.* **2010**, *104*, 185502.
- (32) Ploigt, H.-C.; Brun, C.; Pivetta, M.; Patthey, F.; Schneider, W.-D. Local Work Function Changes Determined by Field Emission Resonances, NaCl/Ag(100). *Phys. Rev. B: Condens. Matter Mater. Phys.* **2007**, *76*, 195404.
- (33) Olsson, F. E.; Paavilainen, s.; Persson, M.; Repp, J.; Meyer, G. Multiple Charge States of Ag Atoms on Ultrathin NaCl films. *Phys. Rev. Lett.* **2007**, *98*, 176803.
- (34) Repp, J.; Meyer, G.; Olsson, F. E.; Persson, M. Controlling the Charge State of Individual Gold Adatoms. *Science* **2004**, *305*, 493–495.
- (35) Kim, S. H.; Jeong, H. G.; Lim, S. J.; Ham, U. D.; Song, Y. J.; Yu, J.; Kuk, Y. Geometric and Electronic Properties of Porphyrin Molecules on Au(111) and NaCl Surfaces. Surf. Sci. 2013, 613, 54–57.
- (36) Yan, S.; Ding, Z.; Xie, N.; Gong, H.; Sun, Q.; Guo, Y.; Shan, X.; Meng, S.; Lu, X. Turning on and off the Rotational Oscillation of a Single Porphine Molecule by Molecular Charge State. *ACS Nano* **2012**, *6*, 4132–4136.
- (37) Cavar, E.; Blum, M.-C.; Pivetta, M.; Patthey, F.; Chergui, M.; Schneider, W.-D. Fluorescence and Phosphorescence from Individual C₆₀ Molecules Excited by Local Electron Tunnelling. *Phys. Rev. Lett.* **2005**, 95, 196102.

- (38) Rossel, F.; Pivetta, M.; Patthey, F.; Cavar, E.; Seitsonen, A. P.; Schneider, W.-D. Growth and Characterization of Fullerene Nanocrystals on NaCl/Au(111). *Phys. Rev. B: Condens. Matter Mater. Phys.* **2011**, *84*, 075426.
- (39) Li, Z.; Chen, H.-Y. T.; Schouteden, K.; Lauwaet, K.; Giordano, L.; Trioni, M. I.; Janssens, E.; Iancu, V.; Van Haesendonck, C.; Lievens, P.; et al. Self-Doping of Ultrathin Insulating Films by Transition Metal Atoms. *Phys. Rev. Lett.* **2014**, *112*, 026102.
- (40) Perdew, J. P.; Burke, K.; Ernzerhof, M. Generalized Gradient Approximation Made Simple. *Phys. Rev. Lett.* **1996**, *77*, 3865–3868.
- (41) Kresse, G.; Hafner, J. Ab Initio Molecular Dynamics for Liquid Metals. *Phys. Rev. B: Condens. Matter Mater. Phys.* **1993**, 47, 558–561.
- (42) Kresse, G.; Furthmüller, J. Efficient Iterative Schemes for Ab Initio Total-Energy Calculations Using A Plane-Wave Basis Set. *Phys. Rev. B: Condens. Matter Mater. Phys.* **1996**, *54*, 11169–11186.
- (43) Blöchl, P. E. Projector Augmented-Wave Method. *Phys. Rev. B: Condens. Matter Mater. Phys.* **1994**, *50*, 17953–17979.
- (44) Lauwaet, K.; Schouteden, K.; Janssens, E.; Van Haesendonck, C.; Lievens, P.; Trioni, M. I.; Giordano, L.; Pacchioni, G. Resolving All Atoms of An Alkali Halide via Nanomodulation of the Thin NaCl Film Surface Using the Au(111) Reconstruction. *Phys. Rev. B: Condens. Matter Mater. Phys.* **2012**, *85*, 245440.
- (45) Bader, R. F. W. A Quantum Theory of Molecular Structure and Its Applications. *Chem. Rev.* (Washington, DC, U.S.) **1991**, 91, 893–928.
- (46) Grimme, S. Semiempirical GGA-Type Density Functional Constructed with a Long-Range Dispersion Correction. *J. Comput. Chem.* **2006**, 27, 1787–1799.
- (47) Mercurio, G.; McNellis, E. R.; Martin, I.; Hagen, S.; Leyssner, F.; Soubatch, S.; Meyer, J.; Wolf, M.; Tegeder, P.; Tautz, F. S.; et al. Structure and Energetics of Azobenzene on Ag(111): Benchmarking Semiempirical Dispersion Correction Approaches. *Phys. Rev. Lett.* **2010**, *104*, 036102.
- (48) Dion, M.; Rydberg, H.; Schroder, E.; Langreth, D. C.; Lundqvist, B. I. Van der Waals Density Functional for General Geometries. *Phys. Rev. Lett.* **2004**, *92*, 246401.
- (49) Klimeš, J.; Bowler, D. R.; Michaelides, A. Chemical Accuracy for the Van Der Waals Density Functional. *J. Phys.: Condens. Matter* **2010**, 22, 022201.
- (50) Yudanov, I.; Pacchioni, G.; Neyman, K.; Rösch, N. Systematic density Functional Study of the Adsorption of Transition Metal Atoms on the MgO(001) Surface. *J. Phys. Chem. B* **1997**, *101*, 2786–2792.
- (51) Neyman, K. M.; Inntam, C.; Nasluzov, V. A.; Kosarev, R.; Rösch, N. Adsorption of d-Metal Atoms on the Regular Mgo(001) Surface: Density Functional Study of Cluster Models Embedded in An Elastic Polarizable Environment. *Appl. Phys. A: Mater. Sci. Process.* **2004**, *78*, 823–828.
- (52) Giordano, L.; Baistrocchi, M.; Pacchioni, G. Bonding of Pd, Ag, and Au Atoms on MgO(100) Surfaces and MgO/Mo(100) Ultra-Thin Films: A Comparative DFT Study. *Phys. Rev. B: Condens. Matter Mater. Phys.* **2005**, 72, 115403–11.
- (53) Gao, W. W.; Baker, T. A.; Zhou, L.; Pinnaduwage, D. S.; Kaxiras, E.; Friend, C. M. Chlorine Adsorption on Au(111): Chlorine Overlayer or Surface Chloride? *J. Am. Chem. Soc.* **2008**, *130*, 3560–3565.
- (54) Shao, X.; Prada, S.; Giordano, L.; Pacchioni, G.; Nilius, N.; Freund, H.-J. Tailoring the Shape of Metal Ad-Particles by Doping the Oxide Support. *Angew. Chem., Int. Ed.* **2011**, *50*, 11525–11527.
- (55) Stavale, F.; Shao, X.; Nilius, N.; Freund, H.-J.; Prada, S.; Giordano, L.; Pacchioni, G. Donor Characteristics of Transition-Metal-Doped Oxides: Cr-Doped MgO versus Mo-Doped CaO. *J. Am. Chem. Soc.* **2012**, *134*, 11380–11383.
- (56) Prada, S.; Giordano, L.; Pacchioni, G. Charging of Gold Atoms on Doped MgO and CaO: Identifying the Key Parameters by DFT Calculations. *J. Phys. Chem. C* **2013**, *117*, 9943–9951.
- (57) These values are obtained with a (2×2) cell and differ slightly from those obtained with a (4×4) cell reported in ref 39.
- (58) Sun, Y. N.; Giordano, L.; Goniakowski, J.; Lewandowski, M.; Qin, Z. H.; Noguera, C.; Shaikhutdinov, S.; Pacchioni, G.; Freund, H.-

J. The Interplay between Structure and CO Oxidation Catalysis on Metal-Supported Ultrathin Oxide Films. *Angew. Chem., Int. Ed.* **2010**, 49, 4418–4421.